Rational gRNA design based on transcription factor binding data

David Bergenholm[1,2,†], Yasaman Dabirian[1,2,†], Raphael Ferreira[1,2,†], Verena Siewers[1,2], Florian David[1,2], and Jens Nielsen[1,2,3,*]

[1]Department of Biology and Biological Engineering, Chalmers University of Technology, Gothenburg, Sweden
[2]Novo Nordisk Foundation Center for Biosustainability, Chalmers University of Technology, Gothenburg, Sweden
[3]Bioinnovation Institute, Copenhagen, Denmark
[†]These authors contributed equally.
*Corresponding author: E-mail: nielsenj@chalmers.se

Abstract

The clustered regularly interspaced short palindromic repeats (CRISPR)/Cas9 system has become a standard tool in many genome engineering endeavors. The endonuclease-deficient version of Cas9 (dCas9) is also a powerful programmable tool for gene regulation. In this study, we made use of *Saccharomyces cerevisiae* transcription factor (TF) binding data to obtain a better understanding of the interplay between TF binding and binding of dCas9 fused to an activator domain, VPR. More specifically, we targeted dCas9–VPR toward binding sites of Gcr1–Gcr2 and Tye7 present in several promoters of genes encoding enzymes engaged in the central carbon metabolism. From our data, we observed an upregulation of gene expression when dCas9–VPR was targeted next to a TF binding motif, whereas a downregulation or no change was observed when dCas9 was bound on a TF motif. This suggests a steric competition between dCas9 and the specific TF. Integrating TF binding data, therefore, proved to be useful for designing guide RNAs for CRISPR interference or CRISPR activation applications.

Key words: transcription factor binding; CRISPRa; *Saccharomyces cerevisiae*; glycolytic promoters; gRNA design

1. Introduction

The clustered regularly interspaced short palindromic repeats (CRISPR)/Cas system, a defense mechanism involved in phage immunity in many bacteria (1), has received considerable attention for its application in genome engineering (2, 3). There are different types of CRISPR systems (4), and the one being mainly employed for genome editing and gene regulation is based on the type II system from *Streptococcus pyogenes*, which uses a single Cas protein, Cas9, together with a single guide RNA (gRNA) (5, 6). The Cas9 protein has been extensively characterized and engineered in several studies, resulting in Cas9 variants with different catalytic properties (7, 8). In one approach, the two nuclease domains were mutated (RuvC^{D10A} and HNH^{H840A}), resulting in a catalytically inactive Cas9, which is often referred to as dCas9 (endonuclease-deficient Cas9) (9, 10). This variant has been widely used as a programmable tool for gene regulation, referred to as CRISPR interference or CRISPR activation (CRISPRi/a). Such regulation enables both the repression of the target gene when dCas9 is expressed as it is or when fused to a repressor domain, such as the mammalian transcriptional repressor domain Mxi (11), and activation when fused to an activator domain, such as the tripartite VPR composed of the three transcriptional activators VP64,

p65 and Rta (12), resulting in a CRISPR-based transcription factor (crisprTF) system. Depending on where in the promoter region the crisprTF binds, different transcriptional regulation can be achieved (13). The impact of crisprTF binding is influenced by several parameters, including the distance to the TATA box (or the TATA-like sequence) or the transcription start site, nucleosome occupancy and intereference with the binding of other TFs in the same region. Achieving predictive and precise gene regulation is, however, challenging, and this is mainly due to the complexity of the regulatory processes and our limited understanding of them (14, 15).

Most TFs in *Saccharomyces cerevisiae* act as activators (16, 17) and are involved in the recruitment of the preinitiation complex and RNA polymerase II, leading to the initiation of gene transcription. Gcr1, Gcr2 and Tye7 are all extensively studied transcriptional activators in yeast. Gcr1 and Gcr2 act as heterodimers, where Gcr1 includes the DNA-binding domain and Gcr2 the activating domain. The heterodimer binds to the consensus motif GGAWGC. Notably, the Gcr1–Gcr2 heterodimer has most of its targets identified in the glycolytic pathway (18–20). Tye7 is a basic helix–loop–helix transcriptional activator with the consensus binding motif (CAT)CACGTG. Most of its targets are also identified in the

glycolytic pathway (21). The colocalization of Gcr1–Gcr2 and Tye7, especially in the glycolytic pathway, has previously been reported (22, 23). One interesting aspect of the TF–DNA interaction is to identify which binding event constitutes a change in gene expression. In combinatorial studies investigating the deletion of both a specific TF gene and its binding sites (BSs), only 10–20% of the TF-targeted genes showed changes in expression levels upon TF gene deletion (24). One reason might be redundancies in the system as many TFs have paralogs, for example, the genes encoding the TFs Fkh1p and Fkh2p. However, with the usage of CRISPRi/a, the importance of a specific TF binding event could potentially be identified through the competition between the TF and dCas9.

In this study, we use previously established high-resolution binding profiles (chromatin immunoprecipitation (ChIP-exo)) for Gcr1–Gcr2 and Tye7. We then use CRISPRa (dCas9–VPR) to target their identified BSs and analyze the effect of this competition.

2. Materials and methods

2.1 Chemicals and reagents

DNA gel extraction and plasmid purification kits were purchased from Thermo Fischer Scientific. The Gibson Assembly® Master mix was purchased from New England Biolabs. Phusion High-Fidelity DNA Polymerase (Thermo Fisher Scientific) was used for polymerase chain reaction amplification. All reagents used for media preparation were purchased from Formedium unless otherwise noted.

2.2 Plasmid and strain construction

Saccharomyces cerevisiae strain CEN.PK113-11C (*MATa SUCMAL2-8^c his3Δ1 ura3-52*) was used as the background strain for transformation with the promoter–green fluorescent protein (GFP) cassettes and the corresponding gRNA plasmids targeting the specific promoters. For standard cloning procedures, competent *Escherichia coli* cells, DH5α, were routinely used. YPD medium, containing 10 g/l yeast extract, 20 g/l casein peptone and 20 g/l glucose, was used when preparing yeast competent cells. For the selection of yeast transformants carrying *URA3*-based plasmids and an *HIS3*-based cassette, synthetic complete medium plates without uracil and histidine containing 6.7 g/l yeast nitrogen base without amino acids, 0.77 g/l complete supplement mixture without uracil and histidine, and 20 agar and 20 g/l glucose were used. For fluorescence measurements, yeast strains were cultured in a defined minimal medium containing 7.5 g/l $(NH_4)_2SO_4$, 14.4 g/l KH_2PO_4, 0.5 g/l $MgSO_4 \cdot 7H_2O$, 20 g/l glucose, 2 ml/l trace metal and 1 ml/l vitamin solution (25). The pH was adjusted to 6.5 with KOH. For culturing *E. coli* cells, lysogenic broth supplemented with 100 mg/l ampicillin was used.

The plasmid containing dCas9–VPR (pERA-109) (26) was used for all the dCas9-based experiments. The gRNAs were designed using Benchling (www.benchling.com), and the sequences can be seen in Supplementary Table S1 in the Supporting Information. The promoter sequences were based on the 1000-bp region upstream the start codon of their respective genes. The promoters were ordered from Twist Bioscience (San Francisco, CA, USA) and cloned into the integrative vector p395 (27) together with GFP and an N-degron, which provided GFP with a half-life of around 70 min, as described previously (28). The N-degron and GFP were ordered as a fragment from Twist Bioscience (San Francisco, CA, USA) and amplified using primers 1 and 2, and

the backbone, p395 vector, was amplified using primers 3 and 4 (Supplementary Table S2, Supporting Information). The respective promoters, N-degron tag and GFP, were assembled into the backbone p395 using the Gibson Assembly Master Mix (New England Biolabs). These resulted in the plasmids pDYR01-10 (Supplementary Table S3, Supporting Information). All plasmids were verified through restriction digestion and sequencing. The plasmids were then digested with NotI for 1 h, and the fragments were transformed into the CEN.PK113-11C background strain. The transformation of the dCas9–VPR-based plasmids pDYR11-55 (Supplementary Table S3, Supporting Information) resulted in the strains DYR001-055 (Supplementary Table S4, Supporting Information).

2.3 Fluorescence measurements

All strains were analyzed in a 48-well FlowerPlate at 1200 rpm, employing a Biolector (m2p-labs GmbH). Cultures were started from a preculture grown for 24 h, at an OD_{600} of 0.1 in 1 ml of minimal medium. For calculating the biomass, scattered light is measured using excitation at 488 nm and emission at 600 nm as well as a gain of 20. For measuring the GFP signal, excitation at 488 nm and emission at 520 nm were used as well
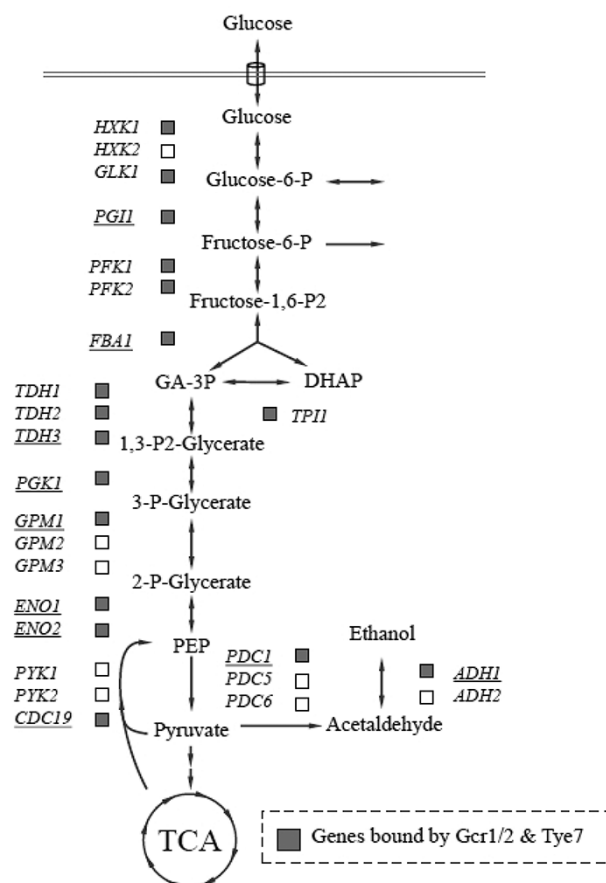

Figure 1. T-rEx-assisted TF identification and targets. We were interested in TFs involved in the central carbon metabolism and found a high correlation between several TFs and respective genes, where especially Gcr1–Gcr2 and Tye7 were shown to be bound to several overlapping genes. Eighteen genes were identified in the core glycolytic pathway, and 10 of these (underscored) were followed up in further experiments.

as a gain of 20. Biological triplicates were used in all experiments; to be able to ensure that the GFP readout was comparable between runs, we included triplicates of several promoters (P_{TDH3} runs 1 and 2, P_{PGK1} runs 1 and 2 and P_{GPM1} runs 1 and 3).

3. Results and discussion

The aim of this study was to better understand the interplay between dCas9 and TF binding in a promoter region. This knowledge could be used to direct the design of gRNAs for CRISPRi/a. In addition, it could also provide information on the importance of specific TF BSs for gene regulation.

To answer this, we used the toolbox T-rEx developed in our lab (https://www.sysbio.se/tools/trex) to analyze the binding of TFs and to perform statistical analysis on the TF bindings. A TF binds to the genome and was assigned a position (peak) if the signal (reads) was higher than the noise (signal-to-noise ratio); the value of this signal-to-noise ratio is then called the peak strength (29). A motif can be identified based on the peak position. Analysis of peak and binding motifs was performed on samples taken from either glucose- or ethanol-limited chemostats as these conditions are most comparable to those of batch cultures in mid-log phase and ethanol phase. We identified three TFs, Gcr1, Gcr2 and Tye7, targeting an overlapping set of genes within the central carbon metabolism (CCM). Out of the 18 genes targeted by all the three TFs Gcr1–Gcr2 and Tye7, we sought to focus on 10 of these genes distributed across the CCM (Figure 1) for further analysis.

Based on this peak and motif identification of the selected genes (Supplementary Table S5, Supporting Information), we targeted these identified TF BSs with dCas9–VPR using three to five rationally designed gRNAs per promoter. These gRNAs either overlapped with the motif of Gcr1–Gcr2 or Tye7 or bound outside of it (Figure 2a). Depending on the location of the protospacer adjacent motif site, the gRNA fully or partially covered the TF binding motif. Additionally, a gRNA target site (20 bp) is commonly longer than the typical motif (8–10 bp), and thus, the gRNA covered not only a motif but also much of the entire binding region and potentially other BSs. gRNA and dCas9–VPR were coexpressed in strains containing one of the selected promoters coupled to a gene encoding GFP (Figure 2a). An example of how the gRNAs were located is shown for the *ENO1* promoter (Figure 2b), where gRNA1 is located on top of a Gcr1–Gcr2 BS, gRNA2 and gRNA3 are located outside of any BS, gRNA4 is located on top of a Tye7 (and Ino2–Ino4) BS and gRNA0 is located close to TATA box. Cells were grown in batch cultivations for 35 h, and their fluorescence was analyzed over time and normalized to the OD. A typical GFP profile of six different strains, five of which were expressing gRNAs, can be seen in Figure 2c. While some gRNAs had no effect (ENO1–21), others resulted in upregulation (ENO1–31) or in downregulation (ENO1–11 and ENO1–41) of GFP expression, where the control represents the expression profile using the *ENO1* promoter with dCas9–VPR expressed but without any gRNA. The normalized fluorescence curves for the remaining promoters can be seen in the Supporting Information (Figure S1), and the raw data can be found in Supporting Information 2.

To investigate the overall gRNA effect, GFP fluorescence data of the strains expressing gRNAs targeted to one of the motifs and strains expressing the nonmotif-targeted gRNAs were separately pooled. Figure 3 shows the fluorescence fold change (FC) of the strains expressing gRNA-binding motifs and nonmotif regions, respectively. A Student's t-test was used on the log2FC to verify whether the binding of gRNAs on certain areas within a promoter resulted in significant changes in fluorescence output. When a gRNA was targeted to one of the motifs, the GFP expression level was either unchanged or decreased, while if bound to a nonmotif region, the GFP expression was increased (Figure 3a). These results indicate the importance of choosing the gRNA site in relation to other TF BSs as they show that binding of dCas9–VPR either on top or outside a TF BS can drastically change its influence on gene transcription. We wanted to look further into the relationship of
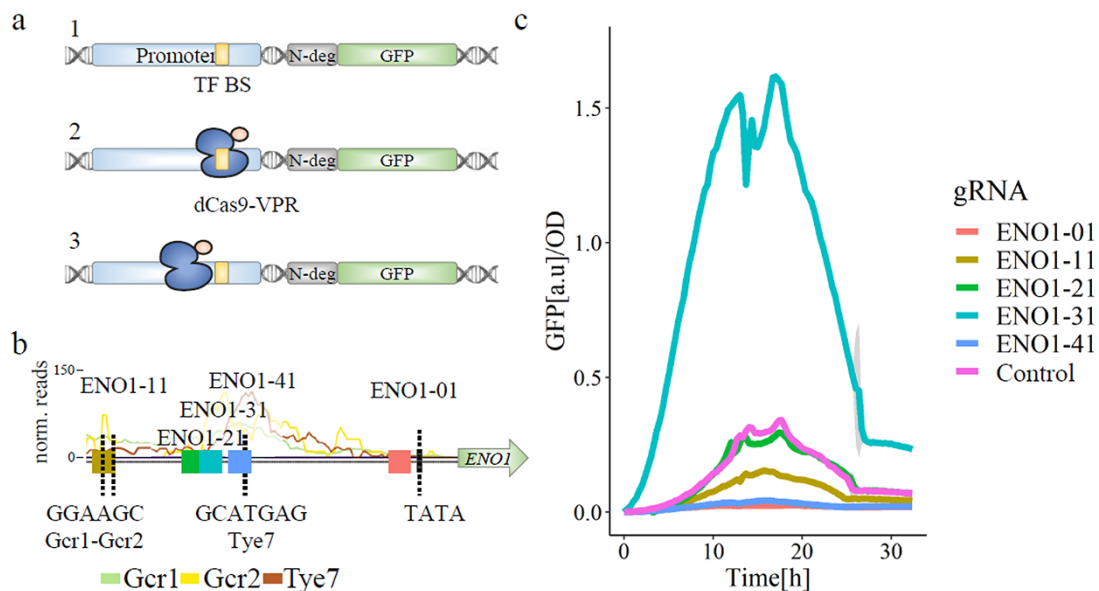

Figure 2. Experimental design and output. (a) Promoter–GFP constructs were coexpressed together with dCas9–VPR in three different scenarios: (1) with no gRNA, (2) with a gRNA targeting a BS of the transcription factors Gcr1–Gcr2 or Tye7 (BS) or (3) with a gRNA targeting a region outside of a TF BS. (b) The *ENO1* promotor with the gRNA target sites and the BSs of either Gcr1–Gcr2 or Tye7 completely or partially covered as well as gRNA sites not located on any BS. (c) Example of fluorescence level over time normalized to OD using GFP coupled to the *ENO1* promoter and the gRNAs expressed from a plasmid encoding also dCas9–VPR.
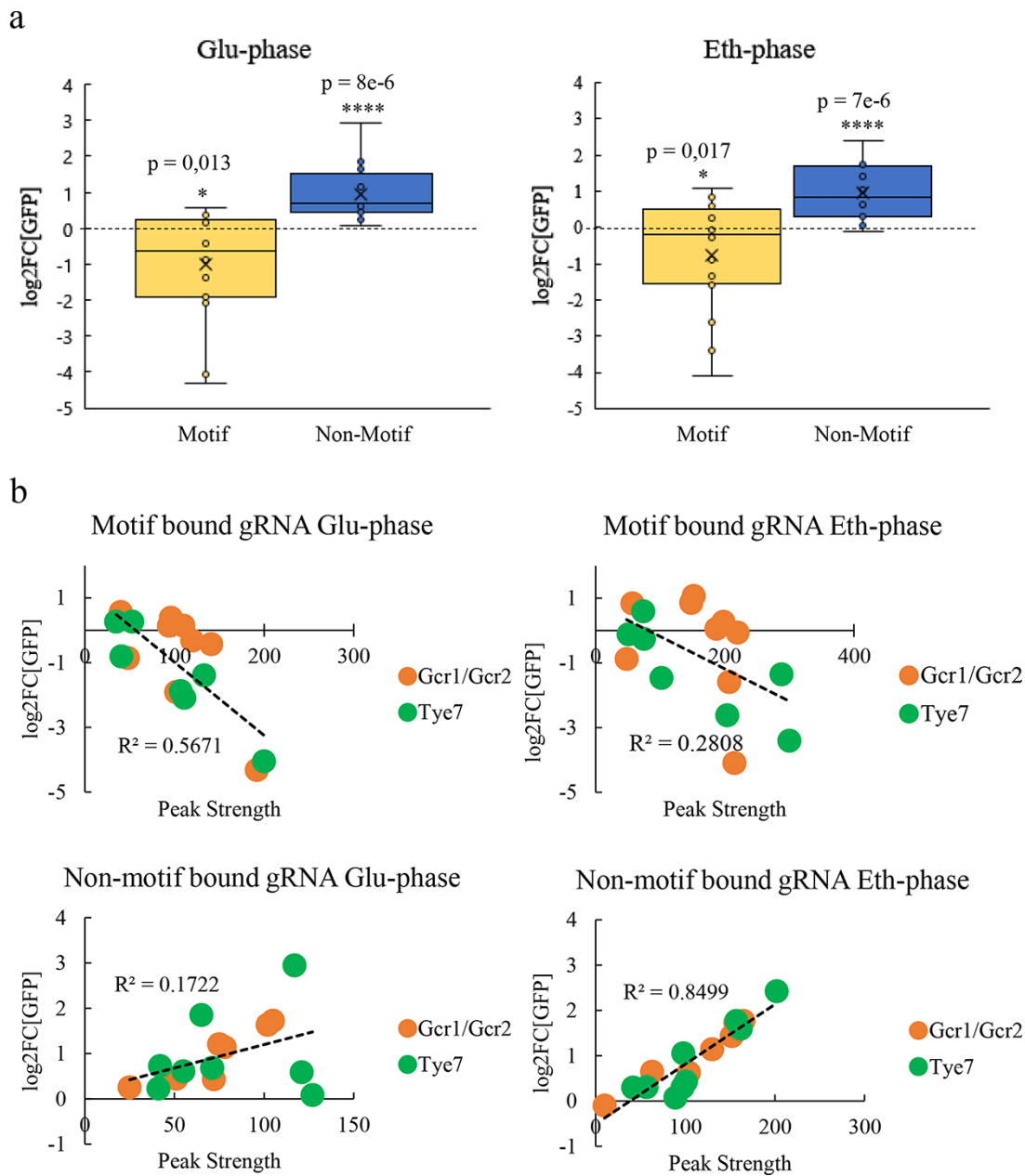
Figure 3. Gene expression changes when targeting dCas9–VPR to a TF motif or nonmotif position. The log2 fold change (log2FC) of the GFP signal is designated to either the motif or the nonmotif group. (a) gRNAs were designed to target motif or nonmotif positions within 10 glycolytic promoters placed upstream of GFP. These motifs are bound by Gcr1, Gcr2 or Tye7. *P* designates the log2FC *P*-value of the Student's t-test. (b) Correlation of the peak strength with the closest transcription factors, BS and the fluorescence, log2FC[GFP], output in each case with binding of gRNA to a motif or nonmotif.

the GFP expression and gRNA BS by taking the binding strength into account.

The peak strength of a TF, i.e. the measure of probability that a TF will occupy a specific site during the ChIP-exo experiment, seems to be correlated with the resulting FC in gene expression when the site was targeted with dCas9–VPR. When a gRNA was targeted close to a high peak strength region, it resulted in a positive FC, while targeting a gRNA to block a high peak strength region, it resulted in a negative FC and the effect increased with increasing peak strength of the TF at this site (Figure 3b). For example, gRNAs bound on Tye7 motifs with peak strengths of 41 and 192 resulted in log2FCs of –0.8 and –4.3, respectively, while

gRNAs bound next to Tye7 motifs with peak strengths of 55 and 105 resulted in log2FCs of 0.6 and 1.7, respectively. In these cases the dCas9–VPR acts as a *de facto* repressor, this by out-competing the endogenous transcription factor. This indicates that dCas9–VPR cannot compensate for the strong activation observed from the native activators. The correlation of the log2FC and the peak strength in the ethanol phase is strong, while for the glucose phase, it is weaker although the same trend can be observed. One should note that the cultivation method for the ChIP-exo experiment (chemostat) and the CRISPRi/a analysis (batch culture) was not the same; however, the same genes were targets under batch cultivations (18–20).
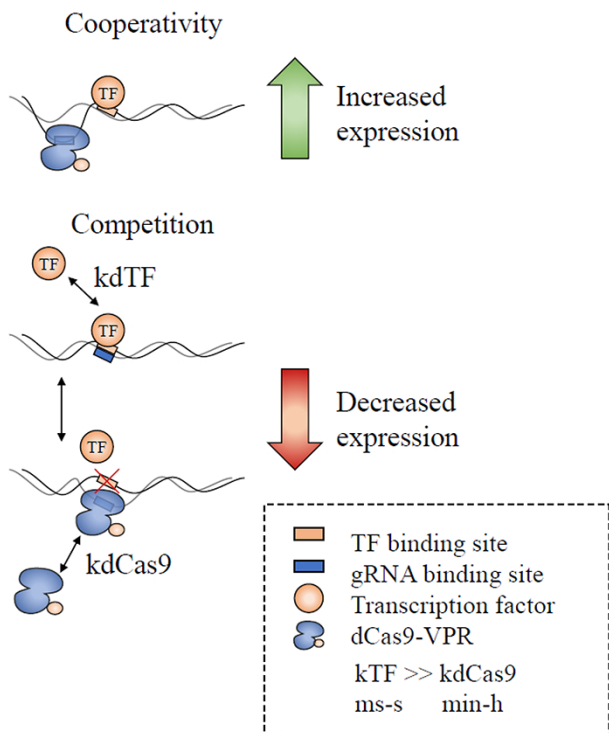
Figure 4. Proposed model of binding cooperativity and competition between dCas9–VPR and an activating TF. Cooperativity: The gRNA site and the TF BS are in close proximity to each other. Cooperativity between the two helps to stabilize the DNA, which leads to a higher activation. The higher the likelihood of TF binding to the BS, the higher the cooperativity effect leading to increased GFP expression. Competition: Targeting the gRNA to the TF BS leads to an instability in the system where the TF and dCas9 compete. The dissociation of dCas9 with the promoter is significantly slower than the dissociation of the TF, which might lead to an almost complete abolishment of TF binding. A lowered expression level for many of these cases indicates that the VPR activation domain is not as efficient as the activation domains on the native TFs.

Nevertheless, these results indicate that there is a direct connection between the binding strength of a TF and the gene expression change resulting from CRISPRi/a, where a negative effect can be seen if the gRNA is bound on top of a TF BS, while we can see a positive effect if the gRNA is bound outside of an activating TF BS. To investigate if the nucleosome occupancy had any effect on the resulting FC, we overlaid nucleosome data adapted from Dang *et al.* (30) with our gRNA BSs, and this showed that there was no difference in nucleosome occupancy between the nonmotif-targeted gRNAs and the motif-targeted gRNAs. Overall, the nucleosome occupancy was low in the tested promoters. Thus, the gRNA binding was most likely not affected by the nucleosome occupancy, and we can, therefore, rule nucleosome occupancy out as an explanation for why the motif targeting led to lower expression levels compared to the targeting of nonmotif regions (Figure S2, Supporting Information). To investigate whether dCas9 perturbs transcription initiation or if there is indeed competition occurring, we looked into the gRNAs that resulted in overexpression to investigate their placement in comparison with the closest motif. If all gRNA target sites that resulted in overexpression were upstream of a motif, this would suggest that the dCas9 was perturbing the transcription. However, we found no such evidence. The gRNAs resulting in overexpression were located both upstream and downstream of motifs (Supplementary Table S5,

Supporting Information). One should note that there are now duplicated promoters in the cell (the endogenous and the inserted reporter promoter), which could cause TF dilution. In a study using the *TDH3* promoter for two different reporters (mRuby2 and Venus), there was, however, no effect seen compared to only using one reporter (mRuby2) (31). The number of gene targets of the TFs ranges from 50 to 330, and we are, therefore, confident that one additional promoter will have low to no dilution effect. It is reported that the residence time of dCas9 and its target DNA is $\sim$206 min (32). This indicates that the dissociation of dCas9 from its DNA target is very weak, whereas a TF has a more dynamic, transient behavior where the dissociation ranges from milliseconds to seconds (33). Thus, a competitive state occurs between the TF and dCas9.

4. Conclusions

We demonstrate that by integrating peak and motif identification from TF data into the gRNA design, one can move one step closer to predictable upregulation or downregulation of genes, even with dCas9 fused to a strong activator system. The strategies used in our study can also be further employed to obtain a more fundamental understanding of the role the activators Gcr1, Gcr2 and Tye7 play and their impact on a given promoter.

Upon binding to the promoter, a TF helps to stabilize the chromatin structure (34), and competition between the TF and the dCas9 might destabilize such a structure. The dissociation of TFs is transient and thus very fast, while the dCas9 has a very slow dissociation. Many TFs act together in a cooperative manner to increase their binding to DNA (35). dCas9 activator has also shown to be cooperative, in the same manner as TFs, when multiple gRNAs have been introduced into the same promoter (36). Similar cooperative mechanisms might be taking place if the dCas9 is bound close to the TF BS, together increasing the expression even further (37). However, if dCas9 competes with the TF, the TF is most likely to be outcompeted by the dCas9 due to the significant differences in dissociation (33, 38). The activation domains of VPR might play an important role in the decrease in expression. In our case, activation mediated by VPR seems to be weaker than the activation from the individual TFs, and so we see less activation when dCas9 is bound on top of the TF BS. Taking these factors together, we propose the model presented in Figure 4.

The underlying principle when designing gRNAs for activation is to bind them in close proximity to a TF motif to obtain a positive effect and far upstream of the TATA box in order to avoid the steric hindrance of the TATA-binding protein, which thereby can prevent the RNA polymerase from initiating transcription. The peak strength of the closest TF is influential to what degree the dCas9 activation can occur, and the stronger the peak strength, the more significant the increase in expression. This might be due to chromatin stabilization from the combined effect, cooperativity, of the TF and dCas9 binding. Binding dCas9 directly on top of a TF BS outcompetes the activating TF, resulting in a decreased expression.

Supplementary data

Supplementary data are available at *SYNBIO* online.

Data availability

Data are available as online supplementary files. The supplementary datasets include supplementary tables and figures, raw data

from fluorescence and OD measurements, gRNA sequences as well as plasmid sequences.

Funding

Conflict of interest statement The authors declare no conflict of interest.

References

1. Jinek,M., Chylinski,K., Fonfara,I., Hauer,M., Doudna,J.A. and Charpentier,E. (2012) A programmable dual-RNA–guided DNA endonuclease in adaptive bacterial immunity. *Science*, **337**, 816–821.
2. Jinek,M., East,A., Cheng,A., Lin,S., Ma,E. and Doudna,J. (2013) RNA-programmed genome editing in human cells. *eLife*, **2**, e00471.
3. Mali,P., Yang,L., Esvelt,K.M., Aach,J., Guell,M., DiCarlo,J.E., Norville,J.E. and Church,G.M. (2013) RNA-guided human genome engineering via Cas9. *Science*, **339**, 823–826.
4. Makarova,K.S., Haft,D.H., Barrangou,R., Brouns,S.J., Charpentier,E., Horvath,P., Moineau,S., Mojica,F.J., Wolf,Y.I., Yakunin,A.F. *et al.* (2011) Evolution and classification of the CRISPR–Cas systems. *Nat. Rev. Microbiol.*, **9**, 467–477.
5. Hsu,P.D., Lander,E.S. and Zhang,F. (2014) Development and applications of CRISPR–Cas9 for genome engineering. *Cell*, **157**, 1262–1278.
6. Doudna,J.A. and Charpentier,E. (2014) The new frontier of genome engineering with CRISPR–Cas9. *Science*, **346**, 1258096.
7. Hu,J.H., Miller,S.M., Geurts,M.H., Tang,W., Chen,L., Sun,N., Zeina,C.M., Gao,X., Rees,H.A., Lin,Z. *et al.* (2018) Evolved Cas9 variants with broad PAM compatibility and high DNA specificity. *Nature*, **556**, 57–63.
8. Slaymaker,I.M., Gao,L., Zetsche,B., Scott,D.A., Yan,W.X. and Zhang,F. (2016) Rationally engineered Cas9 nucleases with improved specificity. *Science*, **351**, 84–88.
9. Qi,L.S., Larson,M., Gilbert,L., Doudna,J., Weissman,J., Arkin,A. and Lim,W. (2013) Repurposing CRISPR as an RNA-guided platform for sequence-specific control of gene expression. *Cell*, **152**, 1173–1183.
10. Perez-Pinera,P., Kocak,D.D., Vockley,C.M., Adler,A.F., Kabadi,A.M., Polstein,L.R., Thakore,P.I., Glass,K.A., Ousterout,D.G., Leong,K.W. *et al.* (2013) RNA-guided gene activation by CRISPR–Cas9-based transcription factors. *Nat. Methods*, **10**, 973–976.
11. Bernards,R. (1995) Transcriptional regulation: flipping the Myc switch. *Current Biol.*, **5**, 859–861.
12. Chavez,A., Scheiman,J., Vora,S., Pruitt,B.W., Tuttle,M., Iyer,E.P.R., Lin,S., Kiani,S., Guzman,C.D., Wiegand,D.J. *et al.* (2015) Highly efficient Cas9-mediated transcriptional programming. *Nat. Methods*, **12**, 326–328.
13. Farzadfard,F., Perli,S.D. and Lu,T.K. (2013) Tunable and multifunctional eukaryotic transcription factors based on CRISPR/Cas.*ACS Synth.Biol.*, **2**, 604–613.
14. Jensen,M.K. (2018) Design principles for nuclease-deficient CRISPR-based transcriptional regulators. *FEMS Yeast Res.*, **18**, 14605.
15. Deaner,M., Mejia,J. and Alper,H.S. (2017) Enabling graded and large-scale multiplex of desired genes using a dual-mode dCas9 activator in *Saccharomyces cerevisiae. ACS Synth.Biol.*, **6**, 1931–1943.
16. Rando,O.J. and Winston,F. (2012) Chromatin and transcription in yeast. *Genetics*, **190**, 351–387.
17. Hahn,S. and Young,E.T. (2011) Transcriptional regulation in *Saccharomyces cerevisiae*: transcription factor regulation and function, mechanisms of initiation, and roles of activators and coactivators. *Genetics*, **189**, 705–736.
18. Sasaki,H. and Uemura,H. (2005) Influence of low glycolytic activities in gcr1 and gcr2 mutants on the expression of other metabolic pathway genes in *Saccharomyces cerevisiae. Yeast*, **22**, 111–127.
19. Uemura,H. and Fraenkel,D.G. (1990) gcr2, a new mutation affecting glycolytic gene expression in *Saccharomyces cerevisiae. Mol. Cell. Biol.*, **10**, 6389–6396.
20. Baker,H.V. (1986) Glycolytic gene expression in *Saccharomyces cerevisiae*: nucleotide sequence of GCR1, null mutants, and evidence for expression. *Mol. Cell. Biol.*, **6**, 3774–3784.
21. Löhning,C. and Ciriacy,M. (1994) The TYE7 gene of *Saccharomyces cerevisiae* encodes a putative bHLH-LZ transcription factor required for Tyl-mediated gene expression. *Yeast*, **10**, 1329–1339.
22. Nishi,K., Park,C.S., Pepper,A.E., Eichinger,G., Innis,M.A. and Holland,M.J. (1995) The GCR1 requirement for yeast glycolytic gene expression is suppressed by dominant mutations in the SGC1 gene, which encodes a novel basic–helix–loop–helix protein. *Mol. Cell. Biol.*, **15**, 2646.
23. Holland,P., Bergenholm,D., Borlin,C.S., Liu,G. and Nielsen,J. (2019). Predictive models of eukaryotic transcriptional regulation reveals changes in transcription factor roles and promoter usage between metabolic conditions. *Nucleic Acids Res.*, **47**, 4986–5000.
24. Gitter,A., Siegfried,Z., Klutstein,M., Fornes,O., Oliva,B., Simon,I. and Bar-Joseph,Z. (2009) Backup in gene regulatory networks explains differences between binding and knockout results. *Mol. Syst. Biol.*, **5**, 276.
25. Verduyn,C., Postma,E., Scheffers,W.A. and Van Dijken,J.P. (1992) Effect of benzoic acid on metabolic fluxes in yeasts: a continuous-culture study on the regulation of respiration and alcoholic fermentation. *Yeast*, **8**, 501–517.
26. Jensen,E.D., Ferreira,R., Jakočiūnas,T., Arsovska,D., Zhang,J., Ding,L., Smith,J.D., David,F., Nielsen,J., Jensen,M.K. *et al.* (2017) Transcriptional reprogramming in yeast using dCas9 and combinatorial gRNA strategies. *Microb. Cell Fact.*, **16**, 46.
27. Jensen,N.B., Strucko,T., Kildegaard,K.R., David,F., Maury,J., Mortensen,U.H., Forster,J., Nielsen,J. and Borodina,I. (2014) EasyClone: method for iterative chromosomal integration of multiple genes *Saccharomyces cerevisiae. FEMS Yeast Res.*, **14**, 238–248.
28. Hackett,E.A., Esch,R.K., Maleri,S. and Errede,B. (2006) A family of destabilized cyan fluorescent proteins as transcriptional reporters in *S. cerevisiae. Yeast*, **23**, 333–349.
29. Bergenholm,D., Liu,G., Holland,P. and Nielsen,J. (2018) Reconstruction of a global transcriptional regulatory network for control of lipid metabolism in yeast by using chromatin immuno-precipitation with lambda exonuclease digestion. *mSystems*, **3**, e00215–17.

30. Dang,W., Sutphin,G., Dorsey,J., Otte,G., Cao,K., Perry,R., Wanat,J., Saviolaki,D., Murakami,C., Tsuchiyama,S. *et al.* (2014) Inactivation of yeast Isw2 chromatin remodeling enzyme mimics longevity effect of calorie restriction via induction of genotoxic stress response. *Cell Metab.*, **19**, 952–966.

31. Lee,M.E., DeLoache,W.C., Cervantes,B. and Dueber,J.E. (2015) A highly characterized yeast toolkit for modular, multipart assembly. *ACS Synth. Biol.*, **4**, 975–986.

32. Ma,H., Tu,L.-C., Naseri,A., Huisman,M., Zhang,S., Grunwald,D. and Pederson,T. (2016) CRISPR-Cas9 nuclear dynamics and target recognition in living cells. *J. Cell Biol.*, **214**, 529–537.

33. Swift,J. and Coruzzi,G.M. (2017) A matter of time—how transient transcription factor interactions create dynamic gene regulatory networks. *Biochimica Et Biophysica Acta. Gene Regulatory Mechanisms*, **1860**, 75–83.

34. Yan,C., Chen,H. and Bai,L. (2018) Systematic study of nucleosome-displacing factors in budding yeast. *Mol. Cell*, **71**, 294–305.e4.

35. Adams,C.C. and Workman,J.L. (1995) Binding of disparate transcriptional activators to nucleosomal DNA is inherently cooperative. *Mol. Cell. Biol.*, **15**, 1405–1421.

36. Perez-Pinera,P., Kocak,D.D., Vockley,C.M., Adler,A.F., Kabadi,A.M., Polstein,L.R., Thakore,P.I., Glass,K.A., Ousterout,D.G., Leong,K.W. *et al.* (2013) RNA-guided gene activation by CRISPR-Cas9-based transcription factors. *Nat. Methods*, **10**, 973–976.

37. Angelici,B., Mailand,E., Haefliger,B. and Benenson,Y. (2016) Synthetic biology platform for sensing and integrating endogenous transcriptional inputs in mammalian cells. *Cell Rep.*, **16**, 2525–2537.

38. Jones,D.L., Leroy,P., Unoson,C., Fange,D., Ćurić,V., Lawson,M.J. and Elf,J. (2017) Kinetics of dCas9 target search in *Escherichia coli*. *Science*, **357**, 1420–1424.